JPET #208223

Title page

Anti-fibrotic and anti-inflammatory activity of the tyrosine kinase inhibitor, nintedanib, in experimental models of lung fibrosis

Lutz Wollin, Isabelle Maillet, Valérie Quesniaux, Alexander Holweg, Bernhard Ryffel

Boehringer Ingelheim Pharma GmbH & Co. KG, Biberach Germany (LW, AH)

UMR7355, INEM, CNRS Orleans, France and IIDMM, University of Cape Town, RSA (IM VQ, BR)

Target Journal: The Journal of Pharmacology and Experimental Therapeutics

This study was funded by Boehringer Ingelheim Pharma GmbH & Co. KG . [no grant number]

Running title page

Running title: Anti-fibrotic and anti-inflammatory activity of nintedanib

Corresponding author:

Lutz Wollin

Boehringer Ingelheim Pharma GmbH & Co. KG, Biberach, Germany

stefan-lutz.wollin@boehringer-ingelheim.com

Tel: +49 (7351) 54-94993 Fax: +49 (7351) 83-94993

Number of text pages: 37

Number of tables: 2

Number of figures: 8 (+ 4 supplementary)

Number of references: 48

Abstract word count: 256

Introduction word count: 612

Discussion word count: 1,446

Abbreviations

ANOVA	Analysis of variance
APC	Antigen presenting cell
BAL	Bronchoalveolar lavage
BALF	Bronchoalveolar lavage fluid
CAB	Chromotrop-anilinblue
ELISA	Enzyme-linked immunosorbent assay
ERK	Extracellular signal-regulated kinases
FACS	Fluorescence-activated cell sorting
FGF(1/2/3)	Fibroblast growth factor 1/2/3
FGFR(1/2/3)	Fibroblast growth factor receptor 1/2/3

GAPDH	Glyceraldehyde 3-phosphate dehydrogenase
HRP	Horseradish peroxidase
IC_{50}	Half-maximal inhibitory concentration
IL-1(β)	Interleukin-1 (beta)
IL-1Ra	Interleukin-1 receptor antagonist (protein)
IL1RN	Interleukin-1 receptor antagonist (gene)
IL-6	Interleukin-6
IPF	Idiopathic pulmonary fibrosis
KC	Keratinocyte chemoattractant
MMP	Matrix metalloproteinase
NHLF	Normal human lung fibroblasts
PBS	Phosphate buffered saline
PCR	Polymerase chain reaction
PDGF BB	Platelet-derived growth factor BB (homodimer)
PDGF(α/β)	Platelet-derived growth factor (alpha/beta)
PDGFR(α/β)	Platelet-derived growth factor receptor (alpha/beta)
RTK	Receptor tyrosine kinase
SDS-PAGE	Sodium dodecyl sulfate polyacrylamide gel electrophoresis
SMA	Smooth muscle actin
TBS	Tris-buffered saline
TGF-β	Transforming growth factor beta
TIMP-1	Tissue inhibitor of metalloproteinase
VEGF	Vascular endothelial growth factor
VEGFR(1/2/3)	Vascular endothelial growth factor receptor 1/2/3

Abstract

The tyrosine kinase inhibitor nintedanib (BIBF 1120) is in clinical development for the treatment of idiopathic pulmonary fibrosis (IPF). To explore its mode of action, nintedanib was tested in human lung fibroblasts and mouse models of lung fibrosis. Human lung fibroblasts expressing PDGF-receptor-α and -β were stimulated with PDGF-BB. Receptor activation was assessed by autophosphorylation and cell proliferation by bromodeoxyuridine incorporation. TGFβ-induced fibroblast to myofibroblast transformation was determined by αSMA mRNA analysis. Lung fibrosis was induced in mice by intratracheal bleomycin or silica particle administration. Nintedanib was administered qd by gavage at 30, 60 or 100 mg/kg. Preventive nintedanib treatment started on the day that bleomycin or silica was administered, therapeutic treatment at various times after the induction of lung fibrosis. Bleomycin caused increased macrophages and lymphocytes in the bronchoalveolar lavage (BAL) and elevated IL-1β, TIMP-1 and collagen in lung tissue. Histology revealed chronic inflammation and fibrosis. Silica-induced lung pathology additionally showed elevated BAL neutrophils, KC levels and granuloma formation. Nintedanib inhibited PDGF-receptor activation, fibroblast proliferation and fibroblast to myofibroblast transformation. Nintedanib significantly reduced BAL lymphocytes and neutrophils but not macrophages. Furthermore, IL-1β, KC, TIMP-1, and lung collagen were significantly reduced. Histological analysis showed significantly diminished lung inflammation, granuloma formation and fibrosis. The therapeutic effect was dependent on treatment start and duration. Nintedanib inhibited receptor tyrosine kinase activation and the proliferation and transformation of human lung fibroblasts and showed anti-fibrotic and anti-inflammatory activity in two animal models of pulmonary fibrosis. These results suggest that nintedanib may impact the progressive course of fibrotic lung diseases like IPF.

Introduction

Idiopathic pulmonary fibrosis (IPF) is a progressive, severely debilitating disease with a high mortality rate (King, Jr., et al., 2011). Mean survival following diagnosis ranges from 2 to 3 years (Raghu, et al., 2011). Even though IPF is considered rare, it is the most common idiopathic interstitial lung disease (ATS and ERS, 2002). The pathomechanisms that result in IPF are not fully understood. It has been hypothesized that injuries of the lung lead to destruction of epithelial alveolar cells, and that the resulting repair process is dysregulated, leading to the proliferation and migration of fibroblasts, transformation to myofibroblasts and excessive collagen deposition within the lung interstitium and alveolar space (Fernandez and Eickelberg, 2012). Progressive fibrosis with stiffening of the lungs leads to dyspnea and cough. The symptoms of IPF limit physical activity and reduce patients' quality of life and independence (De, et al., 2001;Swigris, et al., 2005). Despite high medical need, the latest international guidelines for the management of IPF did not recommend any specific pharmacological treatments for the chronic treatment of IPF (Raghu, et al., 2011).

Nintedanib (BIBF 1120) is a potent intracellular tyrosine kinase inhibitor targeting fibroblast growth factor receptor (FGFR)-1, -2 and -3, platelet derived growth factor receptor (PDGFR)α and β and vascular endothelial growth factor receptor (VEGFR)-1, -2, and -3. Nintedanib also inhibits the Src family tyrosine kinases Lck and Lyn and Flt-3 (Hilberg, et al., 2008). The contribution of inhibition of specific kinases to the mode of action of nintedanib in IPF has not been clarified. However, distinct functions that may impact IPF pathology have been described for specific tyrosine kinases. FGFR1 is expressed on epithelial cells, endothelial cells, smooth muscle cells, myofibroblast-like cells and macrophages in the lungs of patients with IPF, and FGFR2 on smooth muscle cells, myofibroblast-like cells and neutrophils (Inoue, et al., 2002). FGF-2 stimulates proliferation of lung fibroblasts from patients with IPF (Hetzel, et al., 2005). *In vivo* abrogation of FGF signaling reduces bleomycin-induced pulmonary fibrosis and improves survival in bleomycin-treated mice (Yu, et al., 2012). PDGF is produced by alveolar macrophages and epithelial cells (Antoniades, et al., 1990;Bonner,

2004). PDGF is a potent mitogen for fibroblasts (Clark, et al., 1993) and appears to play an essential role in the expansion of myofibroblasts by stimulating proliferation, migration and survival. Elevated levels of PDGF have consistently been observed in the fibrotic lesions of various organs (Bonner, 2004). Myofibroblasts, when too active or too numerous, deposit excessive connective tissue products in the alveolar wall. The result is a distorted alveolar architecture with compromised gas exchange (Katzenstein and Myers, 1998;Kim, et al., 2006;Raghu, et al., 2011). PDGFR-specific tyrosine kinase inhibitors reduce pulmonary fibrosis in animal models of lung fibrosis (Abdollahi, et al., 2005;Aono, et al., 2005;Li, et al., 2009;Rice, et al., 1999;Vuorinen, et al., 2007).

Vascular abnormalities are a common feature in interstitial lung diseases; however the roles of angiogenesis and VEGF signaling in IPF are unclear. It is controversial whether angiogenesis plays a key role in abnormal extracellular matrix remodeling and fibrosis in the lung (King, Jr., et al., 2011;Renzoni, 2004), and extensive temporal and spatial heterogeneity in angiogenesis has been observed in patients with IPF (Farkas and Kolb, 2011). However, experimental overexpression of VEGF in airways induces airway inflammation and remodeling with mucus metaplasia and sub-epithelial fibrosis (Lee, et al., 2011), and VEGF expression correlates with sub-epithelial fibrosis in patients with asthma (Chetta, et al., 2005). Anti-VEGF gene therapy attenuates bleomycin-induced fibrosis in mice (Hamada, et al., 2005).

The results of a Phase II trial of nintedanib (the TOMORROW trial) suggest that 12 months' treatment with nintedanib, at a dose of 150 mg bid, slows decline in lung function, reduces acute exacerbations, and preserves quality of life in patients with IPF, and has an acceptable safety and tolerability profile (Richeldi, et al., 2011). Two Phase III trials of nintedanib in patients with IPF have recently been completed.

The rationale for the *in vitro* and *in vivo* studies presented here was to elucidate the potential mode of action of nintedanib in fibrotic lung diseases like IPF. In this report, we describe anti-inflammatory and anti-fibrotic properties of nintedanib. We provide the cellular kinase profile

of nintedanib and assess effects on the proliferation of fibroblasts. Further, we show that nintedanib reduces inflammation and fibrosis in two animal models of lung fibrosis.

Material and methods

Cellular BA/F3 tyrosine kinase assay

The cellular tyrosine kinase assay was performed by Carna Biosciences Inc., Kobe, Japan. The assay principle builds on the work of Daley & Baltimore (Daley, et al., 1987). Briefly, the proliferation and survival of BA/F3 cells is usually dependent on IL-3. BA/F3 cells were transformed by inducing target kinase dimerization via viral vectors. Proliferation and survival were engineered to become dependent upon maintenance of activity of an introduced specific tyrosine kinase. Inhibition of this tyrosine kinase results in a directly proportional decrease in cell viability, which, as each cell is modified to produce a uniform quantity of luciferase, results in decreased luminescence. Nintedanib (methyl (3Z)-3-[({4-[N-methyl-2-(4-methylpiperazin-1-yl)acetamido]phenyl}amino)(phenyl) methylidene]-2-oxo-2,3-dihydro-1H-indole-6-carboxylate ethane sulfonate salt) was provided by Boehringer Ingelheim Pharma GmbH & Co. KG, Biberach, Germany and was tested at concentrations of 10 nmol/L – 1000 nmol/L on FGFR1-4, PDGFRα/β, VEGFR 1-3, Flt-3, Lck, Lyn and Src.

Inhibition of receptor tyrosine kinase (RTK) phosphorylation and proliferation of normal human lung fibroblasts

Normal human lung fibroblasts (NHLF) (No. AG CC-2512, Lonza, Basel, Switzerland) at passage 6 to 8 were stimulated with recombinant human PDGF-BB (220-BB, R&D Systems, GmbH, Wiesbaden-Nordenstadt, Germany), b-FGF (234-FSE, R&D Systems), or VEGF (293-VE, R&D Systems). Stimulation of the respective receptor phosphorylation was explored by Western blot analysis (data not shown) and ELISA. Fibroblast proliferation was assessed by BrdU incorporation. Because only PDGF-BB stimulation led to a statistically significant increase in RTK phosphorylation of PDGFRα and PDGFRβ and fibroblast proliferation, the pharmacology of nintedanib was only explored on these two receptors.

RTK phosphorylation: Briefly, 24 h after seeding 15,000 NHLF/well with 100 µL/well FBM (No: CC-3131, Lonza.) the cells were grown to about 90% confluence. Cells were starved for

24 h and incubated with nintedanib at 0.128 nmol/L – 10 µmol/L for 30 min. Subsequently, the cells were stimulated with PDGF-BB (50 ng/mL) for 8 min. After lysis the amount of phosphorylated receptor was determined by human phospho-PDGFRα and β ELISA (DuoSet IC, R&D Systems, DYC2114-5 and DYC1767-5, respectively).

Proliferation: 24 h after seeding 2000 NHLF/well cells were grown to about 50% confluence. Cells were starved in FBM medium containing insulin for 24 h, then incubated with nintedanib at 0.3 – 1000 nmol/L for 30 min and stimulated with PDGF-BB at 50 ng/mL for 72 h. Subsequently, BrdU incorporation was determined after 18 h according to manufacturers' instruction (Assay no. 11647229001, Roche, Basel, Switzerland) to determine inhibition of proliferation.

TGF-β-stimulated fibroblast to myofibroblast transformation

The activity of nintedanib on transforming growth factor (TGF)-β2-induced α-smooth muscle actin (SMA) gene expression was explored in primary fibroblast cell lines according to Chaudhary et al. (Chaudhary, et al., 2007). Briefly, human lung fibroblasts from three patients (mixed sex) with lung fibrosis were incubated with TGF-β2 in the presence of nintedanib at concentrations ranging from 30 to 3000 nmol/L. After incubation for 72 h, the gene expression levels of α-SMA were determined by quantitative real-time PCR and normalized relative to endogenous 18S RNA. Data are presented as a percentage of gene expression compared with vehicle alone.

Inhibition of RTK activation *in vivo*

Eight- to ten-week-old C57BL/6 mice (Charles River, Kissleg, Germany) were housed under a 12-h light-dark cycle and received food and water ad libitum. Animal experimentation was conducted in accordance with German national guidelines and regulations. An aqueous solution of nintedanib was prepared by heating to 50°C while stirring. Nintedanib was administered by gavage at 3, 10, 30 and 100 mg/kg (n = 3 per group); 110 minutes later,

animals were anesthetized with 60 mg/kg pentobarbital-sodium and 2.5 mg/kg xylazin i.p.. Five minutes later, recombinant mouse PDGF-BB (ProSpec-Tany TechnoGene Ltd., Ness-Ziona, Israel, 50 µg/animal) or vehicle was administered intratracheally. 5 to 30 min after PDGF-BB stimulation, whole lungs were excised.

Western blot analysis of lung tissue

Frozen lungs were lysed in 1 mL lysis buffer (50 mmol/L Tris-HCl, pH 7.6, 137 mmol/L sodium chloride, 10% glycerol, 0.1% Igepal, 0.1% SDS, 50 mmol/L sodium fluoride, 1 mmol/L sodium orthovanadate) containing protease inhibitor cocktail (Thermo Fisher Scientific, Rockford, IL) using an Ultrathurrax (IKA, Staufen, Germany). Lysates were cleared by centrifugation before total protein determination with the BCA protein assay (Thermo Fisher Scientific GmbH). SDS PAGE and Western blotting were performed following a standard procedure using the Novex NuPAGE system (Life Technologies GmbH, Darmstadt, Germany). Following this, separation proteins were transferred to a PVDF membrane (Millipore, Billerica, MA, USA) in a wet blotting system (Bio-Rad, Hercules, CA, USA). Afterwards membranes were blocked and then probed with antibodies directed against GAPDH, PDGFRβ, phosphorylated PDGFRαβ (Tyr849/Tyr857), phosphorylated ERK1/2 (Thr202/Tyr204), phosphorylated AKT (Ser473) (all Cell Signaling Technologies, Danvers, MA, USA) and PDGFRα (Santa Cruz Biotechnology, Santa Cruz, CA, USA). The membranes were then washed in TBS-T followed by incubation with HRP-conjugated secondary antibodies (Jackson ImmunoResearch Laboratories, West Grove, PA, USA). Immunoreactive bands were detected by addition of an enhanced chemiluminescence substrate (Perkin Elmer, Waltham, MA, USA). The relative signal intensity of each band was determined with the AIDA image analysis software (Raytest) and corrected to the signal intensity of the loading control, GAPDH.

Bleomycin- and silica-induced lung fibrosis in mice

Eight-week-old female C57BL/6 mice (Janvier, Le Genest Saint Isle, France) were kept in groups of five. Animals had access to water and food ad libitum. All animal experiments were

conducted according to the French Government's ethical and animal experiment regulations and the protocols were approved by the Regional Ethics committee (CL2007-021). Nintedanib was administered qd by gavage at 30, 60, or 100 mg/kg/day. Administration volume was 10 mL/kg body weight. Control animals received vehicle only. Depending on the model, animals received a single dose of bleomycin (clinical grade, Bleomycine Bellon, Sanofi-Aventis, France 1, mg = 1000 IU) at 3 mg/kg or silica particles at 2.5 mg/mouse by intranasal instillation as described before (Gasse, et al., 2007;Lo, et al., 2010). Controls received the respective saline solution by intranasal instillation.

The study settings and drug treatment protocols are shown in Table 1. Briefly, in the preventive studies, nintedanib treatment started on the day of bleomycin or silica administration. In the therapeutic studies, nintedanib treatment started after the induction of lung fibrosis when the initial lung injury and inflammation were already abating. In each treatment group, 10 animals were included. All analyses were performed on the last day of the experiment. Lung function was analyzed in the bleomycin study only. For invasive measurement of airway resistance and dynamic lung compliance with a plethysmograph (Buxco, London, UK), mice were anesthetized by intra-peritoneal injection of a solution containing ketamine/xylazine. Lung function testing was done with half the animals (n=5 per group).

Mice were euthanized at the end of the experiment (Table 1). Total cell and differential cell counts were determined in the bronchoalveolar lavage fluid (BALF), total lung collagen was determined in lung tissue by means of the Sircol assay, and IL-1β, IL-6, KC and TIMP-1 were determined in lung homogenates. Details of the methods were according to Gasse et al. (Gasse, et al., 2007).

After BAL and lung perfusion, the large lobe was fixed in 4% buffered formaldehyde and sections of 3 µm were stained with H&E or Chromotrope Aniline Blue. The severity of the morphological changes (infiltration by neutrophils and mononuclear cells and destruction and

thickening of the alveolar septae, and fibrosis and granuloma formation) were assessed semi-quantitatively using a score of 0–5 by two independent observers blinded to the treatments.

Statistics

All data are presented as mean ± S.E.M. of n animals. Statistical differences between groups were analyzed by one-way ANOVA with subsequent Dunnett`s multiple comparison test for all parametric data and Kruscal-Wallis test followed by Dunn's multiple comparison test for non-parametric data (GraphPad Software Inc., GraphPad Prism 5.04, La Jolla, CA). Statistical significance was accepted at $p < 0.05$.

Results

Inhibitory activity of nintedanib on RTKs in a cellular BA/F3 assay

Nintedanib inhibited FGFR1-4, PDGFRα/β, VEGFR 1-3, FLT-3, LCK, LYN and SRC, in a dose-dependent manner in BA/F3 cells engineered to be proliferation-dependent on a single RTK. IC_{50} values for nintedanib are shown in Table 2.

Effect of nintedanib on PDGF-BB-induced PDGFRα and β phosphorylation and proliferation of NHLF

Nintedanib inhibited PDGF-BB-stimulated PDGFRα and β phosphorylation in a concentration-dependent manner with IC_{50} values of 22 nmol/L and and 39 nmol/L, respectively (Fig. 1).

Nintedanib inhibited proliferation of PDGF-BB-stimulated fibroblasts with an IC_{50} value of 64 nmol/L. Complete inhibition of PDGFRαand β phosphorylation led to 70% inhibition of fibroblast proliferation (Fig.1).

Effect of nintedanib on TGF-β-stimulated fibroblast to myofibroblast differentiation

Nintedanib inhibited TGF-β-stimulated fibroblast to myofibroblast differentiation as detected by αSMA gene expression in human fibroblasts from patients with IPF with an IC_{50} of 144 nmol/L (data not shown).

Effect of nintedanib on PDGFR phosphorylation in mouse lungs

PDGFRα and β expression remained quite stable 5 to 30 min after PDGF stimulation (Suppl. Fig. 1). Maximum activation of the PDGFR detected by receptor phosphorylation was noted 5 min after stimulation with PDGF-BB (Suppl. Fig. 1) and maximum downstream signaling of P-AKT and P-ERK was detected at 15 min (Suppl. Fig. 1).

To explore the efficacy of nintedanib to inhibit PDGFR phosphorylation as a marker of receptor activation, nintedanib was dosed orally in mice and 2h later, PDGFR was stimulated

by PDGF-BB. Nintedanib significantly inhibited PDGFR phosphorylation determined 5 min after PDGF stimulation in a dose-dependent manner (Fig. 2A and B). Downstream signaling of P-AKT and P-ERK was also diminished in a dose-dependent manner (Fig. 2A and Suppl. Fig. 2). The expression of PDGFRα and β was slightly elevated at higher doses of nintedanib 5 min after PDGF-BB stimulation (Suppl. Fig. 2).

Effect of nintedanib on pulmonary inflammation and fibrosis in a mouse model of bleomycin-induced lung injury and fibrosis

A single intranasal administration of bleomycin was well tolerated and not associated with clinical adverse effects except for an initial loss of body weight of about 5% in the preventive study and a more sustained loss of up to 10% of body weight, reaching its maximum between day 9 and 11, in the therapeutic study. Bleomycin administration caused a significant increase in lung weight at day 14 in the preventive study (vehicle control, 0.24 ± 0.010 g compared to bleomycin control, 0.32 ± 0.013 g, $P<0.01$) and at day 21 in the therapeutic study (vehicle control, 0.28 ± 0.014 g compared to bleomycin control, 0.41 ± 0.023 g, $P<0.001$). Neither airway resistance nor lung compliance was significantly changed by bleomycin administration at day 14 compared to the vehicle-treated controls (data not shown). In contrast, at day 21 bleomycin administration led to an increase in airway resistance (2.8 ± 0.49 $cmH_2O/mL*s$, $P<0.05$) and a decrease in lung compliance (0.013 ± 0.0028 mL/cmH_2O, $P<0.05$) compared to vehicle-treated animals (1.39 ± 0.059 $cmH_2O/mL*s$ and 0.024 ± 0.0012 mL/cmH_2O, respectively). Nintedanib treatment did not influence lung weight or lung function.

Regardless of whether it was analyzed after 14 days or 21 days, bleomycin administration caused a similar significant increase in total cells (Fig. 3A and 4A), macrophages (Fig. 3B and 4B) and lymphocytes (Fig. 3C and 4C) measured in the BALF, while neutrophils were not detectable in the BALF (data not shown). Nintedanib significantly reduced lymphocyte counts in the preventive study at doses of 30 and 60 mg/kg (Fig. 3C, $P<0.001$) and in the

therapeutic study only at a dose of 60 mg/kg (Fig. 4C, *P*<0.01) but had no effect on total cell (Fig. 3A and 4A) or macrophage counts (Fig. 3B and 4B).

Bleomycin administration significantly increased IL-1β (Fig. 3D and 4D) and TIMP-1 concentrations (Fig. 3F and 4F) determined in lung tissue homogenates compared to controls. The increase in IL-1β was similar at day 14 (Fig. 3D) and day 21 (Fig. 4D). TIMP-1 concentration further increased 1.9-fold between day 14 and day 21 (Fig. 3F and 4F, respectively). IL-1β was normalised by nintedanib in the preventive study (Fig. 3D) and significantly reduced at a dose of 60 mg/kg in the therapeutic study (*P*<0.05, Fig. 4D). Nintedanib reduced TIMP-1 at doses of 30 and 60 mg/kg (Fig. 3F, *P*<0.001) in the preventive study and at a dose of 60 mg/kg (*P*<0.05) in the therapeutic study (Fig. 4F). KC concentrations were not changed (Fig. 3E and 4E).

Bleomycin administration significantly elevated total collagen concentration in lung tissue compared to controls to a similar extent at day 14 and day 21 (Fig. 3G and 4G). Significantly elevated semi-quantitative histology scores indicated inflammation (Fig. 3H and 5B) and fibrosis (Fig. 3I and 6B) at day 14 after bleomycin administration, which was slightly increased at day 21 in the therapeutic study (Fig. 4H, 5F, 4I and 6F). Nintedanib significantly reduced total lung collagen (Fig. 3G), inflammation (Fig. 3H, 5C and D) and fibrosis (Fig. 3I, 6C and 6D) in the preventive study (*P*<0.01, p<0.01 and p<0.05, respectively). In the therapeutic study, the efficacy of nintedanib was slightly reduced (Fig. 4G, 4H) except the significant reduction of the fibrotic score (Fig. 4I, 6G and 6H) (*P*<0.05 and *P*<0.01, respectively).

Effect of nintedanib on pulmonary inflammation, granuloma formation and fibrosis in a mouse model of silica-induced lung injury and fibrosis

Silica administration was also well tolerated and not associated with any clinical adverse effects in mice. Silica administration caused a similar significant increase in lung weight in the preventive study (vehicle control, 0.30 ± 0.037 g compared to silica control, 0.35 ± 0.029 g, *P*<0.01) and in the therapeutic study (vehicle control, 0.29 ± 0.034 g compared to silica

control, 0.36 ± 0.035 g, *P*<0.01). In the preventive study, nintedanib at a dose of 100 mg/kg reduced the silica-induced increase in lung weight by 44%, but this did not reach statistical significance. However, in the therapeutic study, silica-induced lung weight increase was significantly reduced by 74% at a dose of 30 mg/kg (*P*<0.01) and by 86% at a dose of 100 mg/kg (*P*<0.01) if nintedanib treatment was started at day 10. If nintedanib treatment was started at day 20, reductions of 32% at a dose of 30 mg/kg and 43% at a dose of 100 mg/kg were detected (which did not reach statistical significance).

In both the preventive and the therapeutic study, silica administration caused significant increases in total cells (Fig. 7A and 8A), macrophages (Fig. 7B and 8B), lymphocytes (Fig. 7C and 8C) and neutrophils (Fig. 7D and 8D) measured in the BALF (*P*<0.001 for all cell types compared to negative control). Similar to the bleomycin study, nintedanib reduced silica-induced elevation in lymphocyte counts at a dose of 30 mg/kg (Fig. 7C, *P*<0.01) in the preventive study, but not total cell counts (Fig. 7A) or macrophages (Fig. 7B). Neutrophil counts were reduced significantly by nintedanib at doses of 30 and 100 mg/kg (Fig. 7D, *P*<0.01). In the therapeutic study, the significant reduction by nintedanib of lymphocyte count was dependent on dose and start of treatment (Fig. 8C). Higher dose, earlier start of treatment or longer treatment period provided better efficacy. Nintedanib reduced silica-induced neutrophil invasion, but only if treatment was started at day 10 (Fig. 8D, *P*<0.001).

Silica administration significantly increased IL-1β (Fig. 7E and 8E) KC (Fig. 7F and 8F) and TIMP-1 concentrations (Fig. 7G and 8H) determined in lung tissue homogenates to similar extents in both studies compared to saline-treated control lungs (*P*<0.001 for all mediators). IL-6 concentration was only significantly increased in the therapeutic study (Fig. 8G, *P*<0.01). In the preventive study, nintedanib significantly reduced IL-1β (Fig. 7E), KC (Fig. 7F) and TIMP-1 (Fig. 7G) concentrations independent of dose. In the preventive studies, nintedanib reduced IL-1β (Fig. 8E), KC (Fig. 8F), IL-6 (Fig. 8G) and TIMP-1 (Fig. 8H) if treatment was started at day 10, but not if treatment was started at day 20.

Silica administration slightly but significantly elevated total collagen concentration in lung tissue compared to saline-treated controls in both studies (Fig. 7H and 8I). Semi-quantitative analysis of the histology showed that silica administration led to elevated histology scores indicating inflammation (Fig. 7I and 8J), granuloma formation (Fig. 7J and 8K) and fibrosis (Fig. 7K and 8L) in the lungs. Representative histology micrographs are shown as supplementary Figures 3 and 4. Total lung collagen (Fig. 7H), lung inflammation (Fig. 7I), granuloma formation (Fig. 7J) and lung fibrosis (Fig. 7K) were significantly reduced by nintedanib in the preventive study. In the therapeutic study, significant reduction of the pathology by nintedanib was limited to total lung collagen at a dose of 30 mg/kg ($P<0.05$, Fig. 8I), granuloma formation at a dose of 100 mg/kg ($P<0.05$, Fig. 8K) and lung fibrosis at doses of 30 and 100mg/kg ($P<0.05$, Fig. 8L) if treatment was started at day 10, but not if treatment was started at day 20.

Discussion

To improve understanding of the mode of action of nintedanib in fibrotic lung diseases such as IPF, this study explored the inhibitory activity of nintedanib in cellular assays specific for selected tyrosine kinases, in human primary fibroblasts, and in two animal models of pulmonary fibrosis.

A cellular BA/F3 assay confirmed the potent inhibitory activity of nintedanib on PDGFRα and β, VEGFR-2 and -3, and Lck and Lyn and its lower potency on FGFR-3 and 4, as reported in *in vitro* kinase assays (Hilberg, et al., 2008). Differences in IC_{50} values between the cellular BA/F3 assay and the *in vitro* assay were found for FGFR-1 and -2 and for VEGFR-1, with the cellular BA/F3 assay showing lower potency for nintedanib. Since BA/F3 cells are artificially engineered cells, these results can only be taken as a first indication of cellular activity. Compared with the cellular assays in endothelial cells, pericytes and vascular smooth muscle cells described by Hilberg (Hilberg, et al., 2008) the IC_{50} values are in concordance. More important insights were obtained with human lung fibroblasts stimulated with PDGF-BB. PDGF-BB stimulates PDGFRα and β causing αα and ββ homodimerization or αβ heterodimerization (Heldin, et al., 2002) and autophosphorylation of the receptor, which leads to stimulation of fibroblast proliferation (Hetzel, et al., 2005). We demonstrated that nintedanib inhibited PDGFRα and β phosphorylation and proliferation of human lung fibroblasts, an observation that is relevant to the pathology of IPF (Gunther, et al., 2012). The potency of nintedanib was quite similar on all the cellular systems tested, with IC_{50} values ranging from 22 to 64 nmol/L. However, complete inhibition of PDGFRα and β phosphorylation led to only 70% inhibition of fibroblast proliferation, indicating that a proportion of fibroblast proliferation is PDGFR-independent. Nintedanib also inhibited TGFβ-induced fibroblast to myofibroblast differentiation, but only at higher concentrations (IC_{50} = 144 nmol/L).

To show that nintedanib exerts similar effects on PDGFR activation *in vitro* and *in vivo,* we demonstrated that nintedanib dose-dependently inhibited PDGFR phosphorylation and

downstream signaling via P-AKT and P-ERK in mouse lung tissue after oral dosing. Zhuo et al. (Zhuo, et al., 2004) demonstrated that PDGFRα phosphorylation was greater in bleomycin-treated mouse lungs compared with control lungs. Hence, it can be assumed that at least the proliferation of lung fibroblasts activated by PDGF/PDGFR interaction in mice is diminished *in vivo* by the nintedanib doses administered in the bleomycin- and probably in the silica-induced lung fibrosis studies.

The *in vivo* experiments revealed that nintedanib exerted anti-fibrotic activity, as shown by reduced fibrosis in the histological analysis and by diminished lung collagen, reflecting reduced extracellular matrix production and/or deposition. We also found that TIMP-1, a key factor in the fibrogenic response to bleomycin in mice, (Manoury, et al., 2006) was significantly reduced by nintedanib in mouse lung tissue. In general, the anti-fibrotic activity of nintedanib was similar in the preventive and therapeutic studies of the silica-induced and bleomycin-induced fibrosis models except that there was reduced inhibition of TIMP-1 and total lung collagen at a dose of 30 mg/kg in the therapeutic bleomycin study and no inhibitory activity in the therapeutic silica model if nintedanib treatment was started at day 20. Either the late treatment start or the short treatment duration or both could be responsible for the observed reduction in anti-fibrotic activity.

Nintedanib exerted anti-inflammatory activity, demonstrated by reduced lymphocyte and neutrophil counts in the BALF, diminished IL-1β and KC concentrations in lung homogenates, and reduced inflammation and granuloma formation in the histology analysis. In general, the anti-inflammatory activity of nintedanib was weaker in the therapeutic studies than in the preventive studies. This might be related to the fact that in the therapeutic studies, inflammation had peaked before nintedanib treatment was started. Reduction in BALF lymphocyte count seems to be the parameter most sensitive to nintedanib treatment: even though treatment was started late (at day 20) in the therapeutic silica study, nintedanib significantly reduced BALF lymphocytes.

Bleomycin-induced deterioratation in lung function was not influenced by nintedanib in the course of the experiments. This might be related to the relatively short treatment period of 14 days in the preventive as well as in the therapeutic part of the bleomycin study.

The strong and consistent inhibitory activity of nintedanib on IL-1β is an interesting finding. An imbalance of the IL-1 receptor antagonist (IL-1Ra) / IL-1β ratio, resulting in increased IL-1β activity, has been reported in BALF macrophages from patients with IPF (Mikuniya, et al., 1997). Polymorphisms in IL1RN influence IL-1Ra mRNA expression, suggesting that lower levels of IL-1Ra predispose to developing IPF (Korthagen, et al., 2012). IL-1β is a well-known pro-inflammatory cytokine produced by macrophages of IPF patients (Zhang, et al., 1993). IL-1β was shown to have an important role in driving the development of fibrosis (Wilson, et al., 2010). The inhibition of IL-1β by nintedanib may help to dampen the pro-fibrotic milieu in the lung.

A further interesting finding is the significant inhibition of TIMP-1 by nintedanib. TIMP-1 inhibits many MMPs including MMP-1 (also known as collagenase-1) which is capable of degrading type I and II fibrilar collagens (Pardo and Selman, 2012). TIMP-1 expression has been found to be elevated in interstitial macrophages (Selman, et al., 2000), fibroblasts (Ramos, et al., 2001) and sputum (Beeh, et al., 2003) from patients with IPF. Thus the reduction in lung collagen produced by nintedanib might be at least partly attributable to its inhibitory activity on TIMP-1.

Although in this study, only the inhibitory activity of nintedanib on PDGFR was explored *in vitro,* it is likely that inhibition of other tyrosine kinases contributes to the efficacy of nintedanib *in vivo*. According to Hilberg et al, (Hilberg, et al., 2008) exposure in mice after oral administration of 60 and 100 mg/kg nintedanib is sufficient to inhibit FGFRs, VEGFRs, Lck, Src and Flt-3 in the animal experiments presented here. The integrated anti-fibrotic and anti-inflammatory activity of nintedanib might be dependent on its inhibitory activity on multiple kinases. It is well documented that the PDGF/PDGFR signaling cascade is implicated in the development of pulmonary fibrosis (Bonner, 2004) but inhibition of FGFRs

might also have a role in the *in vivo* efficacy of nintedanib. Enhanced FGF levels, as well as increased expression of FGFR1 on epithelial, endothelial, and smooth muscle cell/myofibroblast-like cells and increased expression of FGFR2 on interstitial cells, have been detected in the lungs of patients with IPF (Inoue, et al., 2002). *In vivo* abrogation of FGF signaling has been shown to reduce bleomycin-induced pulmonary fibrosis and improve survival in bleomycin-treated mice (Yu, et al., 2012). The role of VEGF in IPF remains to be further explored but experimental evidence in rats suggests that inhibition of VEGFR may reduce fibrosis (Hamada, et al., 2005). No specific role in the pathology of IPF has been described for Lck, Src and Flt-3. However, anti-inflammatory effects of nintedanib could potentially be partly attributable to its inhibitory activity on these tyrosine kinases (Das, et al., 2006).

No animal model is available resembling the exact pathology and chronicity of human IPF. In our attempt to elucidate the mode of action of nintedanib, inhibitory activity was explored in two well-described animal models of lung inflammation and fibrosis: the bleomycin-induced (Gasse, et al., 2007) and the silica-induced model (Lo, et al., 2010). Both these models reflect at least some aspects of the pathology seen in patients with IPF. When designing our studies, we followed the recommendations of Moeller et al. (Moeller, et al., 2008) in that all potential anti-fibrotic compounds should be evaluated in the phase of established fibrosis, rather than in the early period of bleomycin-induced inflammation, for assessment of antifibrotic properties.

Both models show similarities but also differences in lung pathology. The bleomycin model is reported to show initial lung injury with strong but transient neutrophilic inflammation subsequently leading to lung fibrosis (Izbicki, et al., 2002). Bleomycin is metabolised in the lung, leading to a decrease in neutrophilic inflammation and a fibrotic response that spontaneously resolves after 2-3 months (Walters and Kleeberger, 2008). In the silica model, the stimulating crystals are not cleared from the lung, leading to ongoing inflammation, granuloma formation and progressive fibrosis (Callis, et al., 1985; Brass, et al., 2012). In our

study, lung inflammation and fibrotic score were quite similar in both models except for the strong neutrophilic inflammation and granuloma formation only detected in the silica-treated lungs and the stronger increase in lung weight in the bleomycin-treated lungs, which might be related to stronger matrix deposition indicated by the higher lung collagen increase. The consistent inhibitory effects shown by nintedanib in both animal models suggest that the anti-fibrotic activity demonstrated in this study is an intrinsic feature of nintedanib and not only an indirect activity caused by suppressing the initial inflammatory response.

In summary, we have shown that nintedanib inhibits RTK activation and proliferation and transformation of human lung fibroblasts. *In vivo* nintedanib showed consistent anti-fibrotic and anti-inflammatory activity in two animal models that reflect aspects of pulmonary fibrotic diseases. We propose that the anti-fibrotic and anti-inflammatory activities demonstrated in this study are likely aspects of the mode of action of nintedanib in fibrotic lung diseases. The inhibitory activity of nintedanib on lung fibrosis in the therapeutic studies raises the hope that nintedanib might reduce disease progression in patients with lung fibrosis. The anti-fibrotic and anti-inflammatory activity of nintedanib may impact the clinical course of pulmonary fibrotic diseases like IPF.

Acknowledgements:

Lung fibroblasts from patients with IPF were kindly provided by Prof. J. Müller-Quernheim, University Hospital Freiburg, Germany. The excellent technical assistance of Verena Brauchle and Angela Ostermann (Respiratory Diseases Research, Boehringer Ingelheim Pharma GmbH & Co. KG, Biberach an der Riss, Germany) is gratefully acknowledged. Editorial assistance, supported financially by Boehringer Ingelheim Pharma GmbH & Co KG, was provided by Wendy Morris of Fleishman-Hillard Group, Ltd during the preparation of this manuscript.

Authorship contributions:

Design of the experiments: Wollin, Quesniaux, Holweg, Ryffel

Conducted experiments: Wollin, Holweg, Maillet, Ryffel

Analysis and interpretation of data: All authors

Manuscript preparation: Written by Wollin; revised by Maillet, Quesniaux, Holweg, Ryffel,

Final approval of manuscript: All authors

Reference List

Abdollahi A, Li M, Ping G, Plathow C, Domhan S, Kiessling F, Lee LB, McMahon G, Grone HJ, Lipson KE and Huber PE (2005) Inhibition of platelet-derived growth factor signaling attenuates pulmonary fibrosis. *J Exp Med* **201**:925-935.

American Thoracic Society/European Respiratory Society (2002) International Multidisciplinary Consensus Classification of the Idiopathic Interstitial Pneumonias. This joint statement of the American Thoracic Society (ATS), and the European Respiratory Society (ERS) was adopted by the ATS board of directors, June 2001 and by the ERS Executive Committee, June 2001. *Am J Respir Crit Care Med* **165**:277-304.

Antoniades HN, Bravo MA, Avila RE, Galanopoulos T, Neville-Golden J, Maxwell M and Selman M (1990) Platelet-derived growth factor in idiopathic pulmonary fibrosis. *J Clin Invest* **86**:1055-1064.

Aono Y, Nishioka Y, Inayama M, Ugai M, Kishi J, Uehara H, Izumi K and Sone S (2005) Imatinib as a novel antifibrotic agent in bleomycin-induced pulmonary fibrosis in mice. *Am J Respir Crit Care Med* **171**:1279-1285.

Beeh KM, Beier J, Kornmann O and Buhl R (2003) Sputum matrix metalloproteinase-9, tissue inhibitor of metalloprotinease-1, and their molar ratio in patients with chronic obstructive pulmonary disease, idiopathic pulmonary fibrosis and healthy subjects. *Respir Med* **97**:634-639.

Bonner JC (2004) Regulation of PDGF and its receptors in fibrotic diseases. *Cytokine Growth Factor Rev* **15**:255-273.

Brass DM, Spencer JC, Li Z, Potts-Kant E, Reilly SM, Dunkel MK, Latoche JD, Auten RL, Hollingsworth JW and Fattman CL (2012) Innate immune activation by inhaled lipopolysaccharide, independent of oxidative stress, exacerbates silica-induced pulmonary fibrosis in mice. *PLoS ONE* **7**:e40789.

Callis AH, Sohnle PG, Mandel GS, Wiessner J and Mandel NS (1985) Kinetics of inflammatory and fibrotic pulmonary changes in a murine model of silicosis. *J Lab Clin Med* **105**:547-553.

Chaudhary NI, Roth GJ, Hilberg F, Muller-Quernheim J, Prasse A, Zissel G, Schnapp A and Park JE (2007) Inhibition of PDGF, VEGF and FGF signalling attenuates fibrosis. *Eur Respir J* **29**:976-985.

Chetta A, Zanini A, Foresi A, D'Ippolito R, Tipa A, Castagnaro A, Baraldo S, Neri M, Saetta M and Olivieri D (2005) Vascular endothelial growth factor up-regulation and bronchial wall remodelling in asthma. *Clin Exp Allergy* **35**:1437-1442.

Clark JG, Madtes DK and Raghu G (1993) Effects of platelet-derived growth factor isoforms on human lung fibroblast proliferation and procollagen gene expression. *Exp Lung Res* **19**:327-344.

Daley GQ, McLaughlin J, Witte ON and Baltimore D (1987) The CML-specific P210 bcr/abl protein, unlike v-abl, does not transform NIH/3T3 fibroblasts. *Science* **237**:532-535.

Das J, Chen P, Norris D, Padmanabha R, Lin J, Moquin RV, Shen Z, Cook LS, Doweyko AM, Pitt S, Pang S, Shen DR, Fang Q, de Fex HF, McIntyre KW, Shuster DJ, Gillooly KM, Behnia K, Schieven GL, Wityak J and Barrish JC (2006) 2-aminothiazole as a novel kinase inhibitor template. Structure-activity relationship studies toward the discovery of N-(2-chloro-6-methylphenyl)-2-[[6-[4-(2-hydroxyethyl)-1- piperazinyl)]-2-methyl-4-pyrimidinyl]amino)]-1,3-thiazole-5-carboxamide (dasatinib, BMS-354825) as a potent pan-Src kinase inhibitor. *J Med Chem* **49**:6819-6832.

De VJ, Kessels BL and Drent M (2001) Quality of life of idiopathic pulmonary fibrosis patients. *Eur Respir J* **17**:954-961.

Farkas L and Kolb M (2011) Pulmonary microcirculation in interstitial lung disease. *Proc Am Thorac Soc* **8**:516-521.

Fernandez IE and Eickelberg O (2012) New cellular and molecular mechanisms of lung injury and fibrosis in idiopathic pulmonary fibrosis. *Lancet* **380**:680-688.

Gasse P, Mary C, Guenon I, Noulin N, Charron S, Schnyder-Candrian S, Schnyder B, Akira S, Quesniaux VF, Lagente V, Ryffel B and Couillin I (2007) IL-1R1/MyD88 signaling and the inflammasome are essential in pulmonary inflammation and fibrosis in mice. *J Clin Invest* **117**:3786-3799.

Gunther A, Korfei M, Mahavadi P, von der BD, Ruppert C and Markart P (2012) Unravelling the progressive pathophysiology of idiopathic pulmonary fibrosis. *Eur Respir Rev* **21**:152-160.

Hamada N, Kuwano K, Yamada M, Hagimoto N, Hiasa K, Egashira K, Nakashima N, Maeyama T, Yoshimi M and Nakanishi Y (2005) Anti-vascular endothelial growth factor gene therapy attenuates lung injury and fibrosis in mice. *J Immunol* **175**:1224-1231.

Heldin CH, Eriksson U and Ostman A (2002) New members of the platelet-derived growth factor family of mitogens. *Arch Biochem Biophys* **398**:284-290.

Hetzel M, Bachem M, Anders D, Trischler G and Faehling M (2005) Different effects of growth factors on proliferation and matrix production of normal and fibrotic human lung fibroblasts. *Lung* **183**:225-237.

Hilberg F, Roth GJ, Krssak M, Kautschitsch S, Sommergruber W, Tontsch-Grunt U, Garin-Chesa P, Bader G, Zoephel A, Quant J, Heckel A and Rettig WJ (2008) BIBF 1120: triple angiokinase inhibitor with sustained receptor blockade and good antitumor efficacy. *Cancer Res* **68**:4774-4782.

Inoue Y, King TE, Jr., Barker E, Daniloff E and Newman LS (2002) Basic fibroblast growth factor and its receptors in idiopathic pulmonary fibrosis and lymphangioleiomyomatosis. *Am J Respir Crit Care Med* **166**:765-773.

Izbicki G, Segel MJ, Christensen TG, Conner MW and Breuer R (2002) Time course of bleomycin-induced lung fibrosis. *Int J Exp Pathol* **83**:111-119.

Katzenstein AL and Myers JL (1998) Idiopathic pulmonary fibrosis: clinical relevance of pathologic classification. *Am J Respir Crit Care Med* **157**:1301-1315.

Kim DS, Park JH, Park BK, Lee JS, Nicholson AG and Colby T (2006) Acute exacerbation of idiopathic pulmonary fibrosis: frequency and clinical features. *Eur Respir J* **27**:143-150.

King TE, Jr., Pardo A and Selman M (2011) Idiopathic pulmonary fibrosis. *Lancet* **378**:1949-1961.

Korthagen NM, van Moorsel CH, Kazemier KM, Ruven HJ and Grutters JC (2012) IL1RN genetic variations and risk of IPF: a meta-analysis and mRNA expression study. *Immunogenetics* **64**:371-377.

Lee CG, Ma B, Takyar S, Ahangari F, Delacruz C, He CH and Elias JA (2011) Studies of vascular endothelial growth factor in asthma and chronic obstructive pulmonary disease. *Proc Am Thorac Soc* **8**:512-515.

Li M, Abdollahi A, Grone HJ, Lipson KE, Belka C and Huber PE (2009) Late treatment with imatinib mesylate ameliorates radiation-induced lung fibrosis in a mouse model. *Radiat Oncol* **4**:66.

Lo RS, Dumoutier L, Couillin I, Van VC, Yakoub Y, Uwambayinema F, Marien B, van den BS, Van SJ, Uyttenhove C, Ryffel B, Renauld JC, Lison D and Huaux F (2010) IL-17A-producing gammadelta T and Th17 lymphocytes mediate lung inflammation but not fibrosis in experimental silicosis. *J Immunol* **184**:6367-6377.

Manoury B, Caulet-Maugendre S, Guenon I, Lagente V and Boichot E (2006) TIMP-1 is a key factor of fibrogenic response to bleomycin in mouse lung. *Int J Immunopathol Pharmacol* **19**:471-487.

Mikuniya T, Nagai S, Shimoji T, Takeuchi M, Morita K, Mio T, Satake N and Izumi T (1997) Quantitative evaluation of the IL-1 beta and IL-1 receptor antagonist obtained from BALF macrophages in patients with interstitial lung diseases. *Sarcoidosis Vasc Diffuse Lung Dis* **14**:39-45.

Moeller A, Ask K, Warburton D, Gauldie J and Kolb M (2008) The bleomycin animal model: a useful tool to investigate treatment options for idiopathic pulmonary fibrosis? *Int J Biochem Cell Biol* **40**:362-382.

Pardo A and Selman M (2012) Role of matrix metaloproteases in idiopathic pulmonary fibrosis. *Fibrogenesis Tissue Repair* **5 Suppl 1**:S9.

Raghu G, Collard HR, Egan JJ, Martinez FJ, Behr J, Brown KK, Colby TV, Cordier JF, Flaherty KR, Lasky JA, Lynch DA, Ryu JH, Swigris JJ, Wells AU, Ancochea J, Bouros D, Carvalho C, Costabel U, Ebina M, Hansell DM, Johkoh T, Kim DS, King TE, Jr., Kondoh Y, Myers J, Muller NL, Nicholson AG, Richeldi L, Selman M, Dudden RF, Griss BS, Protzko SL and Schunemann HJ (2011) An official ATS/ERS/JRS/ALAT statement: idiopathic pulmonary fibrosis: evidence-based guidelines for diagnosis and management. *Am J Respir Crit Care Med* **183**:788-824.

Ramos C, Montano M, Garcia-Alvarez J, Ruiz V, Uhal BD, Selman M and Pardo A (2001) Fibroblasts from idiopathic pulmonary fibrosis and normal lungs differ in growth rate, apoptosis, and tissue inhibitor of metalloproteinases expression. *Am J Respir Cell Mol Biol* **24**:591-598.

Renzoni EA (2004) Neovascularization in idiopathic pulmonary fibrosis: too much or too little? *Am J Respir Crit Care Med* **169**:1179-1180.

Rice AB, Moomaw CR, Morgan DL and Bonner JC (1999) Specific inhibitors of platelet-derived growth factor or epidermal growth factor receptor tyrosine kinase reduce pulmonary fibrosis in rats. *Am J Pathol* **155**:213-221.

Richeldi L, Costabel U, Selman M, Kim DS, Hansell DM, Nicholson AG, Brown KK, Flaherty KR, Noble PW, Raghu G, Brun M, Gupta A, Juhel N, Kluglich M and du Bois RM (2011) Efficacy of a tyrosine kinase inhibitor in idiopathic pulmonary fibrosis. *N Engl J Med* **365**:1079-1087.

Selman M, Ruiz V, Cabrera S, Segura L, Ramirez R, Barrios R and Pardo A (2000) TIMP-1, -2, -3, and -4 in idiopathic pulmonary fibrosis. A prevailing nondegradative lung microenvironment? *Am J Physiol Lung Cell Mol Physiol* **279**:L562-L574.

Swigris JJ, Kuschner WG, Jacobs SS, Wilson SR and Gould MK (2005) Health-related quality of life in patients with idiopathic pulmonary fibrosis: a systematic review. *Thorax* **60**:588-594.

Vuorinen K, Gao F, Oury TD, Kinnula VL and Myllarniemi M (2007) Imatinib mesylate inhibits fibrogenesis in asbestos-induced interstitial pneumonia. *Exp Lung Res* **33**:357-373.

Walters DM and Kleeberger SR (2008) Mouse Models of Bleomycin-Induced Pulmonary Fibrosis, in *Current Protocols in Pharmacology* p 46.1-46.17, John Wiley & Sons, Inc..

Wilson MS, Madala SK, Ramalingam TR, Gochuico BR, Rosas IO, Cheever AW and Wynn TA (2010) Bleomycin and IL-1beta-mediated pulmonary fibrosis is IL-17A dependent. *J Exp Med* **207**:535-552.

Yu ZH, Wang DD, Zhou ZY, He SL, Chen AA and Wang J (2012) Mutant Soluble Ectodomain of Fibroblast Growth Factor Receptor-2 IIIc Attenuates Bleomycin-Induced Pulmonary Fibrosis in Mice. *Biol Pharm Bull* **35**:731-736.

Zhang Y, Lee TC, Guillemin B, Yu MC and Rom WN (1993) Enhanced IL-1 beta and tumor necrosis factor-alpha release and messenger RNA expression in macrophages from idiopathic pulmonary fibrosis or after asbestos exposure. *J Immunol* **150**:4188-4196.

Zhuo Y, Zhang J, Laboy M and Lasky JA (2004) Modulation of PDGF-C and PDGF-D expression during bleomycin-induced lung fibrosis. *Am J Physiol Lung Cell Mol Physiol* **286**:L182-L188.

Footnotes

This study was funded by Boehringer Ingelheim Pharma GmbH & Co. KG . [no grant number].

Figure legends

Figure 1. Nintedanib inhibits PDGF-BB-stimulated PDGFRα and β phosphorylation and proliferation of human lung fibroblasts. Human lung fibroblasts were incubated with nintedanib at different concentrations and stimulated with PDGF-BB (50 ng/mL). PDGFRα and β phosphorylation was determined by ELISA specific for the phosphorylated receptors. Proliferation was determined by BrdU incorporation. Concentration–dependent inhibition of PDGFRα (◆) and β (O) autophosphorylation and fibroblast proliferation (■) is presented as mean ± SEM (n = 3 experiments).

Figure 2. Nintedanib inhibits PDGF-BB stimulated PDGFR phosphorylation in mouse lung tissue. C57BL/6 mice received vehicle or 100, 30, 10 and 3 mg/kg of nintedanib by gavage (n = 3 per group). Two hours after compound dosing, PDGF-BB (50 µg) was intratracheally instilled to induce PDGF receptor phosphorylation. Five minutes later, the animals were euthanized and total lungs were excised, lysed and used for Western blot analysis to detect total and phosphorylated PDGF receptors, as well as phosphorylation of the downstream signaling molecules AKT and ERK1/2 by specific antibodies. GAPDH was used as a control. One representative Western blot showing 1 animal from each group is depicted for each antibody analyzed (A). The relative signal intensity of the phosphorylated PDGFRαβ bands was evaluated by densitometry and corrected by the intensity of the GAPDH control. Data are presented as mean ± S.E.M of 3 animals per group. (B). Statistical analysis was performed in Prism Graph Pad using one-way ANOVA with subsequent Dunnett's multiple comparison test *$P < 0.05$; **$P < 0.01$.

Figure 3. Preventive nintedanib treatment reduces bleomycin-induced lung inflammation and fibrosis. C57Bl/6 mice received an intranasal instillation of NaCl or bleomycin 3 mg/kg. Nintedanib was administered qd by gavage at 30 and 60 mg/kg for 14 days. Analyses were performed at day 14. BAL cell differentiation is expressed as cells per mouse lung. A, total cell count, B, macrophages, C, lymphocytes. Mediator concentrations in whole lung homogenates were determined by ELISA. D, interleukin-1 beta (IL-1β), E, chemokine (C-X-C

motif) ligand 1/keratinocyte chemoattractant (KC), F, tissue inhibitor of metalloproteinase-1 (TIMP-1). Total lung collagen was determined by sircol assay in lung homogenate (G). Hematoxylin & eosin and chromotrop-anilinblue (CAB) trichrome stained slices of the left lung were semi-quantitatively scored for inflammation (H) and fibrosis (I), respectively. All groups (n=10 per group) were compared versus bleomycin-treated control animals by ANOVA followed by Dunnett's multiple comparison test for parametric data and Kruskal-Wallis test followed by Dunn's multiple comparison test for non-parametric data. *P<0.05, **P<0.01, ***P<0.001. Values are presented as mean ± S.E.M.

Figure 4. Therapeutic nintedanib treatment reduces bleomycin-induced lung inflammation and fibrosis. C57Bl/6 mice received an intranasal instillation of NaCl or bleomycin 3 mg/kg. Nintedanib was administered qd by gavage at 30 and 60 mg/kg starting at day 7. Analyses were performed at day 21. BAL cell differentiation is expressed as cells per mouse lung. A, total cell count, B, macrophages, C, lymphocytes. D, interleukin-1 beta (IL-1b), E, chemokine (C-X-C motif) ligand 1/keratinocyte chemoattractant (KC), F, tissue inhibitor of metalloproteinase-1 (TIMP-1). Total lung collagen was determined by sircol assay in lung homogenate (G). Hematoxylin & eosin and chromotrop-anilinblue (CAB) trichrome stained slices of the left lung were semi-quantitatively scored for inflammation (H) and fibrosis (I), respectively. All groups (n=10 per group except FACS analysis where n=5) were compared versus bleomycin-treated control animals by ANOVA followed by Dunnett's multiple comparison test for parametric data and Kruskal-Wallis test followed by Dunn's Multiple comparison test for non-parametric data. *P<0.05, **P<0.01, ***P<0.001. Values are presented as mean ± S.E.M.

Figure 5. Nintedanib treatment reduces bleomycin-induced lung inflammation and fibrosis. Representative micrographs of hematoxylin and eosin-stained lung sections from mice of the treatment groups are shown. C57Bl/6 mice that received an intranasal instillation of bleomycin 3 mg/kg (B, F) showed a prominent peri-bronchial and interalveolar inflammation that was absent in control animals (A, E). Nintedanib was administered qd by gavage at 30

(C, G) and 60 mg/kg (D, H). Daily nintedanib treatment from day 0 to day 14 in the preventive study (C-D), and from day 7 till day 21 in the therapeutic study (G-H) reduced bleomycin-induced lung pathology. Analyses were performed on the last day of the study, which was day 14 (A-D) or day 21 (E-H).

Figure 6. Nintedanib treatment reduces bleomycin-induced lung inflammation and fibrosis. Representative micrographs of Chromotrope Aniline Blue-stained lung sections from mice of the treatment groups are shown. C57Bl/6 mice that received an intranasal instillation of bleomycin 3 mg/kg (B, F) showed a prominent peri-brochial and peri-vascular collagen accumulation and peri-bronchial and interalveolar inflammation that was absent in control animals (A, E). Nintedanib was administered qd by gavage at 30 (C, G) and 60 mg/kg (D, H). Daily nintedanib treatment from day 0 to day 14 in the preventive study (C-D), and from day 7 till day 21 in the therapeutic study (G-H) reduced bleomycin-induced lung pathology. Analyses were performed on the last day of the study, which was day 14 (A-D) or day 21 (E-H).

Figure 7. Preventive nintedanib treatment reduces silica-induced lung inflammation and fibrosis. C57Bl/6 mice received an intranasal instillation of NaCl or silica particles 2.5 mg/animal. Nintedanib was administered qd by gavage at 30 and 100 mg/kg for 30 days. Analyses were performed at day 30. BAL cell differentiation is expressed as cells per mouse lung. A, total cell count, B, macrophages, C, lymphocytes, D, neutrophils. Mediator concentrations in whole lung homogenates were determined by ELISA. E, interleukin-1 beta (IL-1b), F, chemokine (C-X-C motif) ligand 1/keratinocyte chemoattractant (KC), G, tissue inhibitor of metalloproteinase-1 (TIMP-1). Total lung collagen was determined by sircol assay in lung homogenate (H). Hematoxylin & eosin and chromotrop-anilinblue (CAB) trichrome stained slices of the left lung were semi-quantitatively scored for inflammation (I), granuloma formation (J) and fibrosis (K). All groups (n=10 per group) were compared versus silica-treated control animals by ANOVA followed by Dunnett's multiple comparison test for

parametric data and Kruskal-Wallis test followed by Dunn's Multiple comparison test for non-parametric data. *P<0.05, **P<0.01, ***P<0.001. Values are presented as mean ± S.E.M.

Figure 8. Therapeutic nintedanib treatment reduces silica-induced lung inflammation and fibrosis. C57Bl/6 mice received an intranasal instillation of NaCl or silica particles 2.5 mg/animal. Nintedanib was administered qd by gavage at 30 and 100 mg/kg starting at day 10 (clear bars) or day 20 (hatched bars). Analyses were performed at day 30. BAL cell differentiation is expressed as cells per mouse lung. A, total cell count, B, macrophages, C, lymphocytes, D, neutrophils. Mediator concentrations in whole lung homogenates were determined by ELISA. E, interleukin-1 beta (IL-1b), F, chemokine (C-X-C motif) ligand 1/keratinocyte chemoattractant (KC), G, interleukin-6 (IL-6), H, tissue inhibitor of metalloproteinase-1 (TIMP-1). Total lung collagen was determined by sircol assay in lung homogenate (I). Hematoxylin & eosin and chromotrop-anilinblue (CAB) trichrome stained slices of the left lung were semi-quantiatively scored for inflammation (J), granuloma formation (K) and fibrosis (L), respectively. All groups (n=10 per group) were compared versus silica-treated control animals by ANOVA followed by Dunnett's multiple comparison test for parametric data and Kruskal-Wallis test followed by Dunn's Multiple comparison test for non-parametric data. *P<0.05, **P<0.01, ***P<0.001. Values are presented as mean ± S.E.M.

Tables:

Table 1. Study settings and treatment protocols of the *in vivo* experiments.

Table 1

Study	Bleomycin-induced lung fibrosis		Silica-induced lung fibrosis	
Posology	once daily, oral			
Model	preventive	therapeutic	preventive	therapeutic
Dose [mg/kg]	30, 60	30, 60	30, 100	30, 100
Study duration [days]	14	21	30	30
Compound administration [days]	0-14	7-21	0-30	10-30 20-30

Table 2

Table 2. Tyrosine kinase inhibition of nintedanib in a cellular BA/F3 assay.

To compare the cellular activity of nintedanib on specific tyrosine kinase receptors, it was tested at 10 nmol/L – 1000 nmol/L in BA/F3 cells engineered to be proliferation-dependent on a single tyrosine kinase. IC_{50} values for nintedanib to inhibit cell proliferation dependent on specific tyrosine kinases are listed in nmol/L.

Assay	IC_{50} [nmol/L]
FGFR1	300-1000
FGFR2	257
FGFR3	300-1000
FGFR4	300-1000
PDGFRα	41
PDGFRβ	58
VEGFR1	300-1000
VEGFR2	46
VEGFR3	33
LCK	22
LYN	300-1000
SRC	811
FLT-3	17

Figure 1

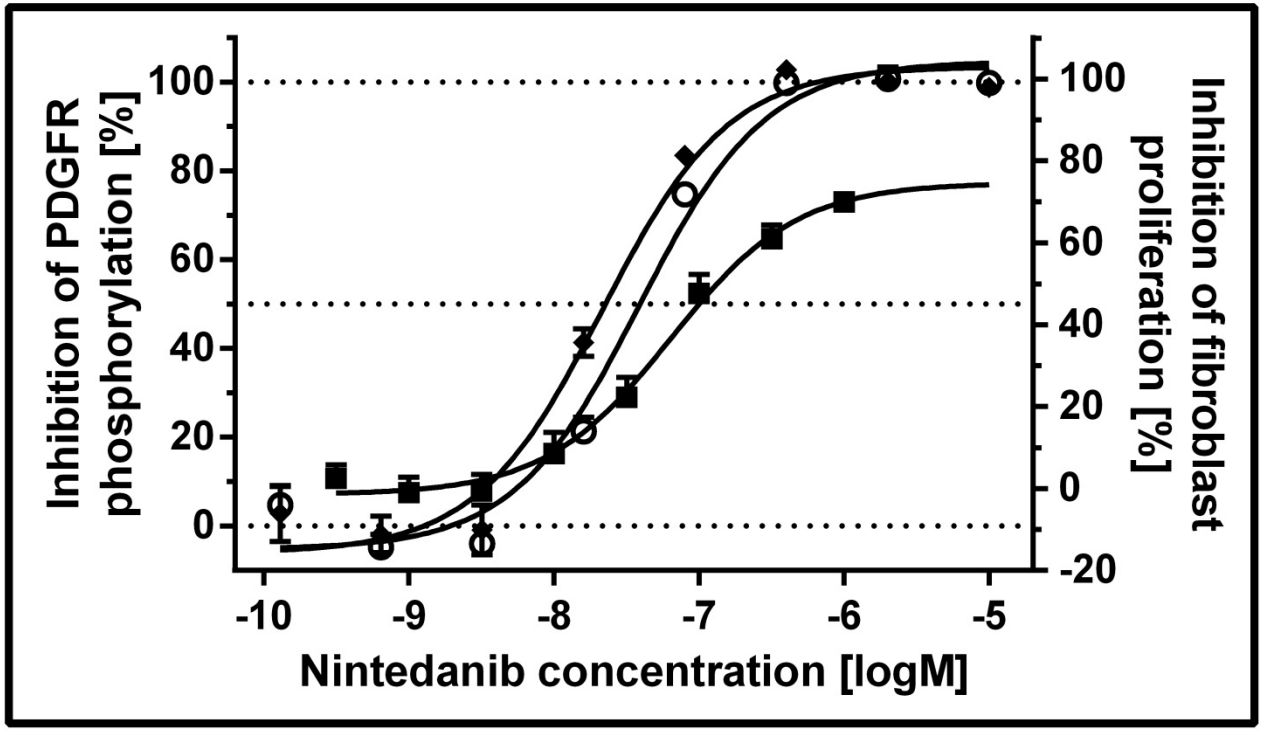
Inhibition of PDGFR phosphorylation [%]
100
80
60
40
20
0
-10
-9
-8
-7
-6
-5
Nintedanib concentration [logM]
100
80
60
40
20
0
-20
Inhibition of fibroblast proliferation [%]

Figure 2A

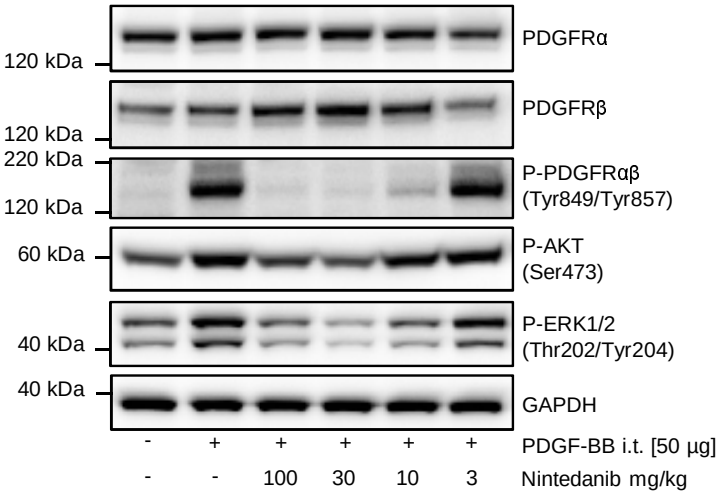
120 kDa
PDGFRα
120 kDa
PDGFRβ
220 kDa
120 kDa
P-PDGFRαβ
(Tyr849/Tyr857)
60 kDa
P-AKT
(Ser473)
40 kDa
P-ERK1/2
(Thr202/Tyr204)
40 kDa
GAPDH
- + + + + +
PDGF-BB i.t. [50 µg]
- - 100 30 10 3
Nintedanib mg/kg

Figure 2B

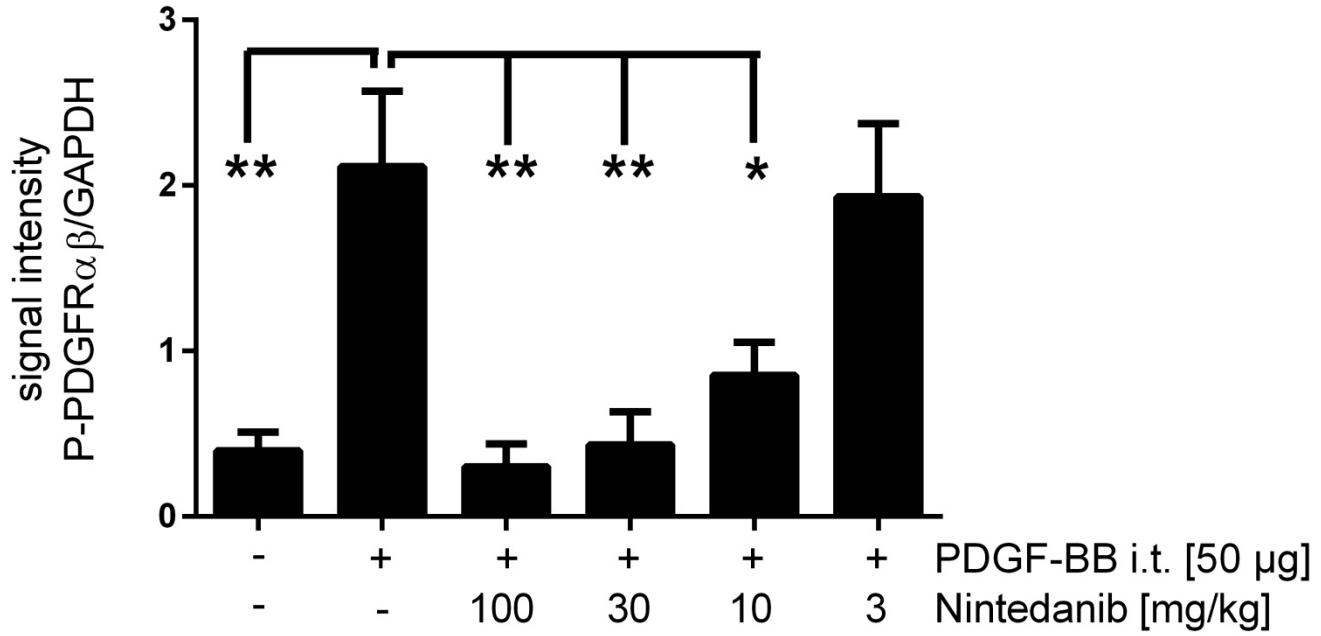
signal intensity
P-PDGFRαβ/GAPDH
3
2
1
0
**
**
**
*
- + + + + + PDGF-BB i.t. [50 µg]
- - 100 30 10 3 Nintedanib [mg/kg]

Figure 3

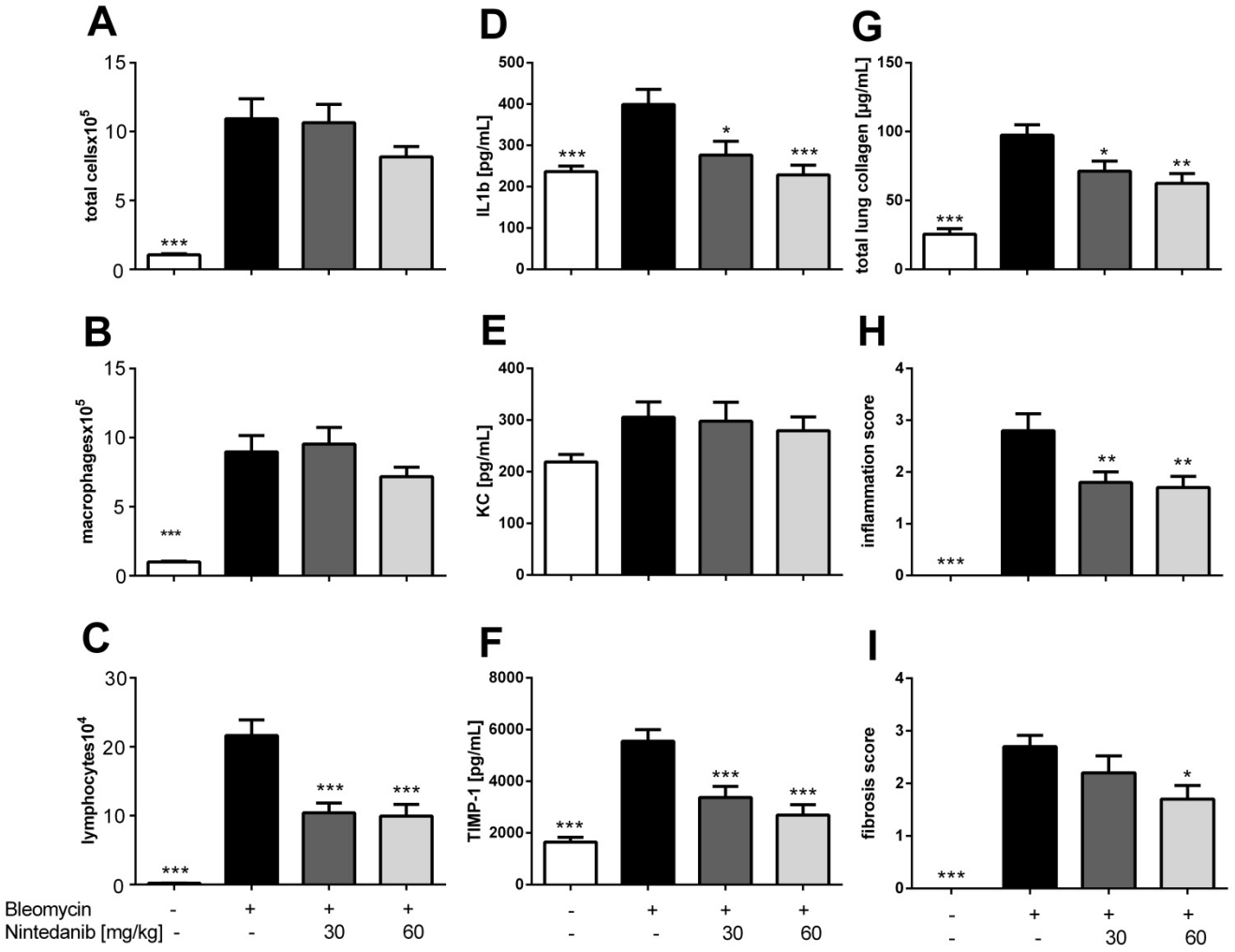
A
total cellsx10^5
B
macrophagesx10^5
C
lymphocytes10^4
D
IL1b [pg/mL]
E
KC [pg/mL]
F
TIMP-1 [pg/mL]
G
total lung collagen [µg/mL]
H
inflammation score
I
fibrosis score
Bleomycin
Nintedanib [mg/kg]

Figure 4

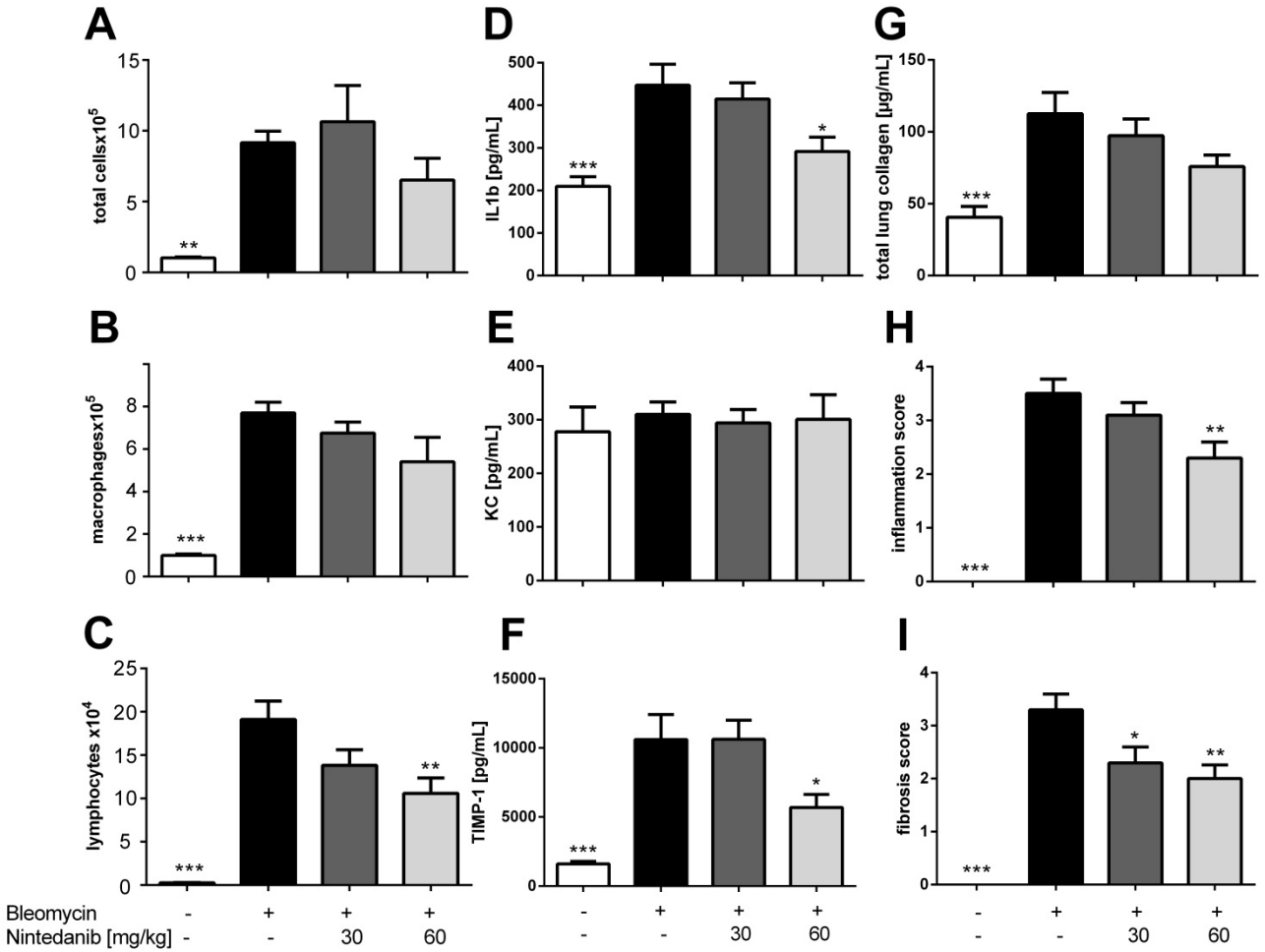
A
total cellsx10^5
15
10
5
0
**
B
macrophagesx10^5
8
6
4
2
0
***
C
lymphocytes x10^4
25
20
15
10
5
0
***
**
D
IL1b [pg/mL]
500
400
300
200
100
0
***
*
E
KC [pg/mL]
400
300
200
100
0
F
TIMP-1 [pg/mL]
15000
10000
5000
0
***
*
G
total lung collagen [µg/mL]
150
100
50
0
***
H
inflammation score
4
3
2
1
0
***
**
I
fibrosis score
4
3
2
1
0
***
*
**
Bleomycin - + + +
Nintedanib [mg/kg] - - 30 60

Figure 5A-D

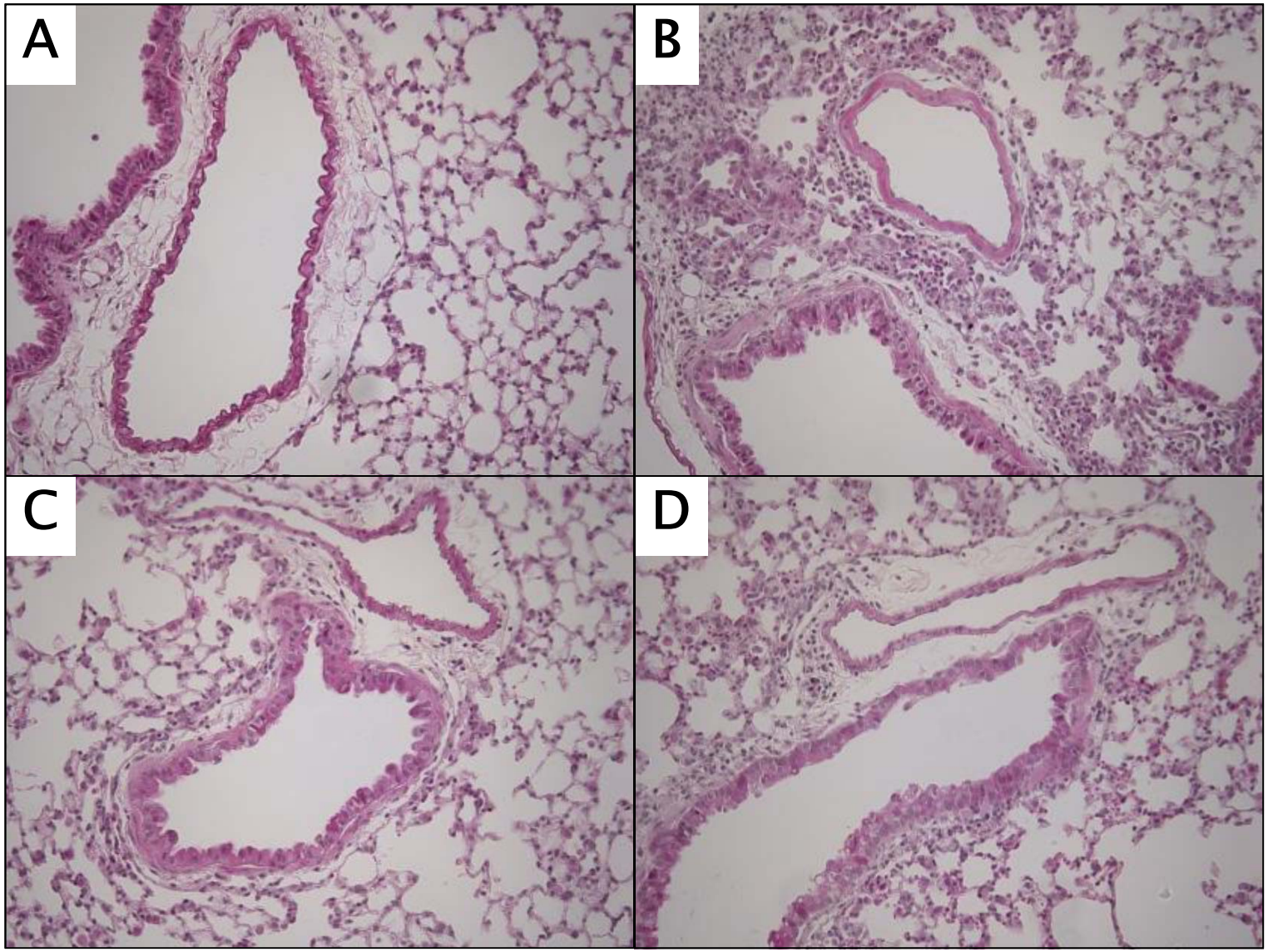

Figure 5E-H

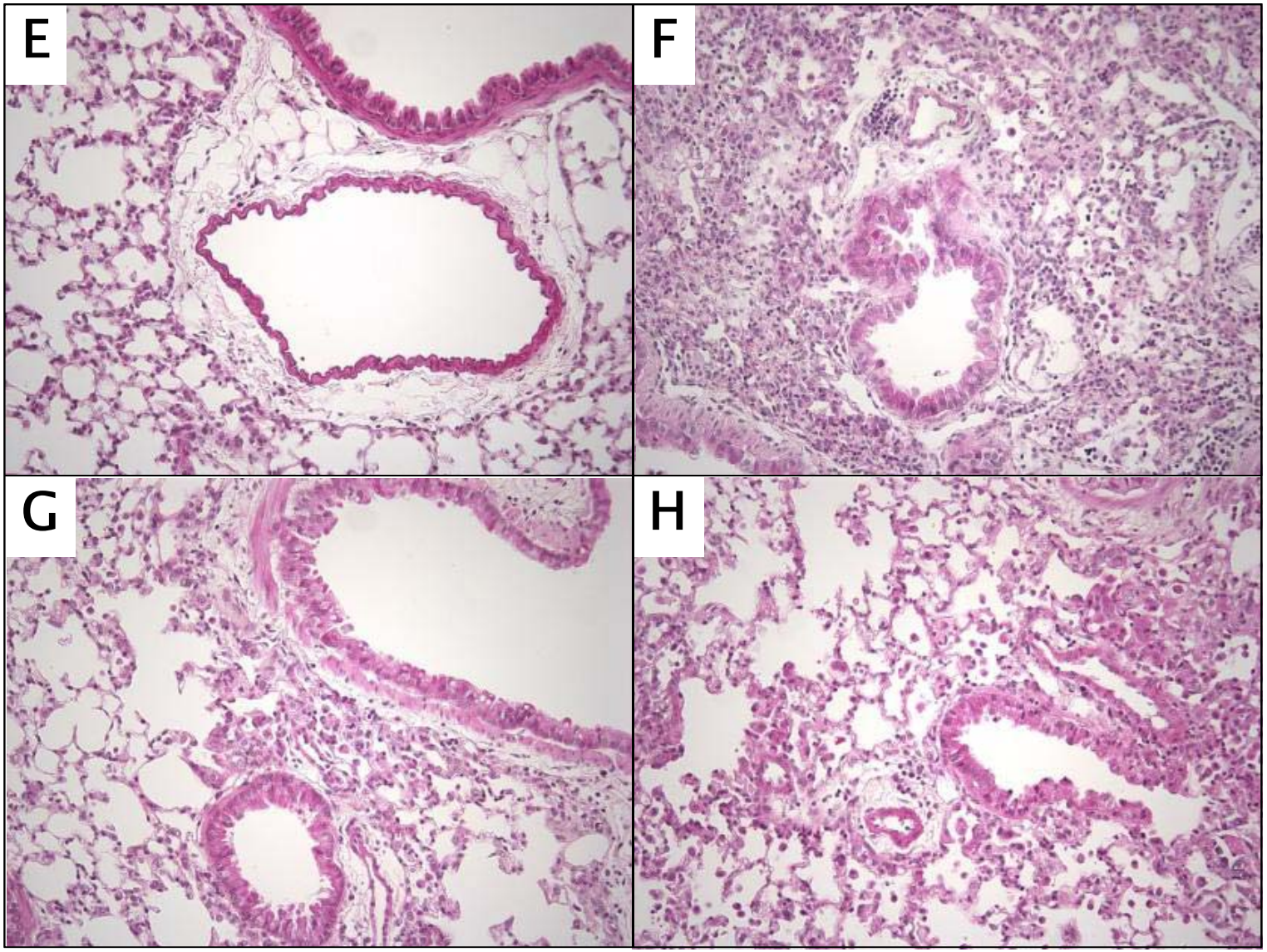

Figure 6A-D

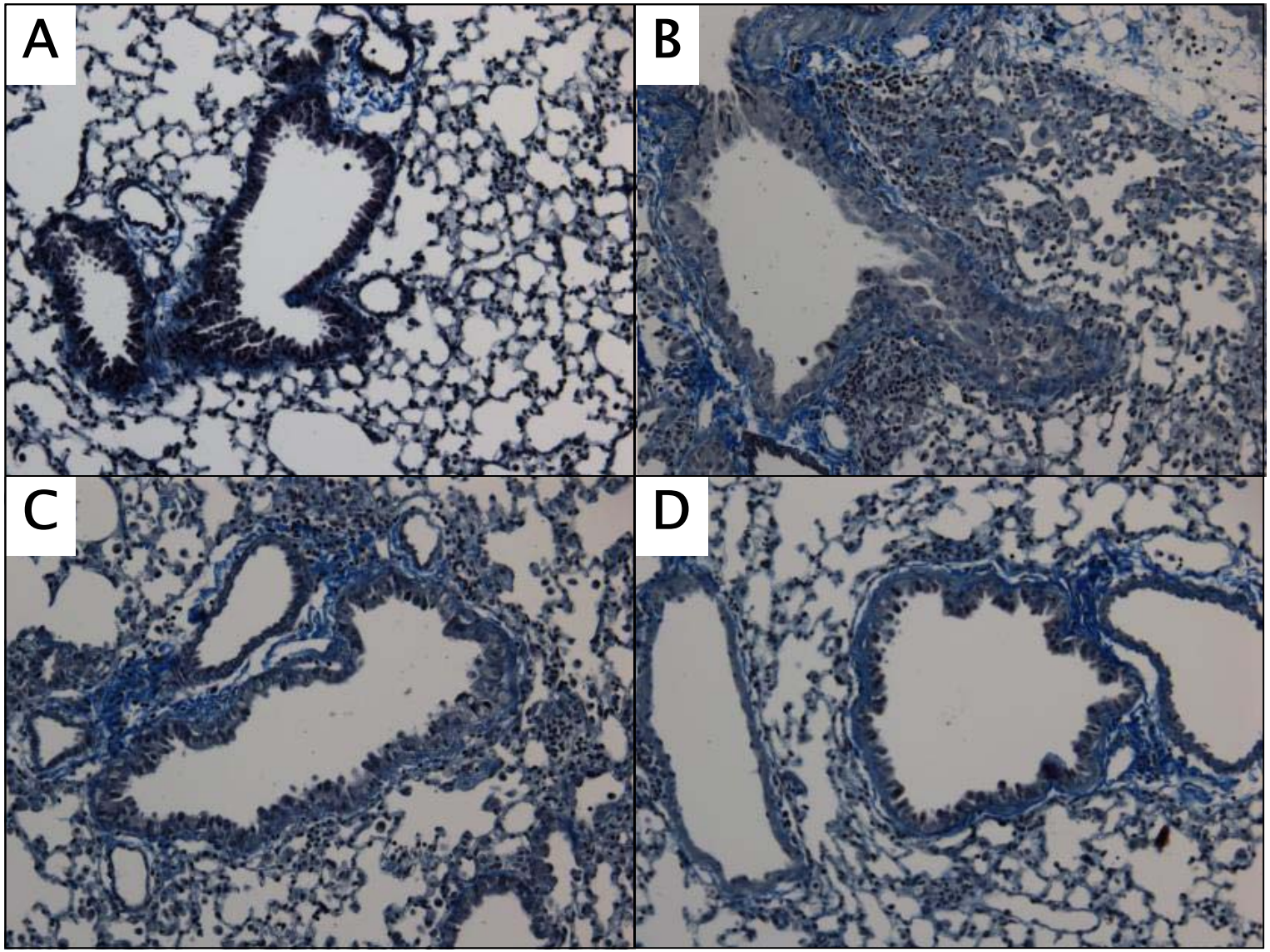

Figure 6E-H

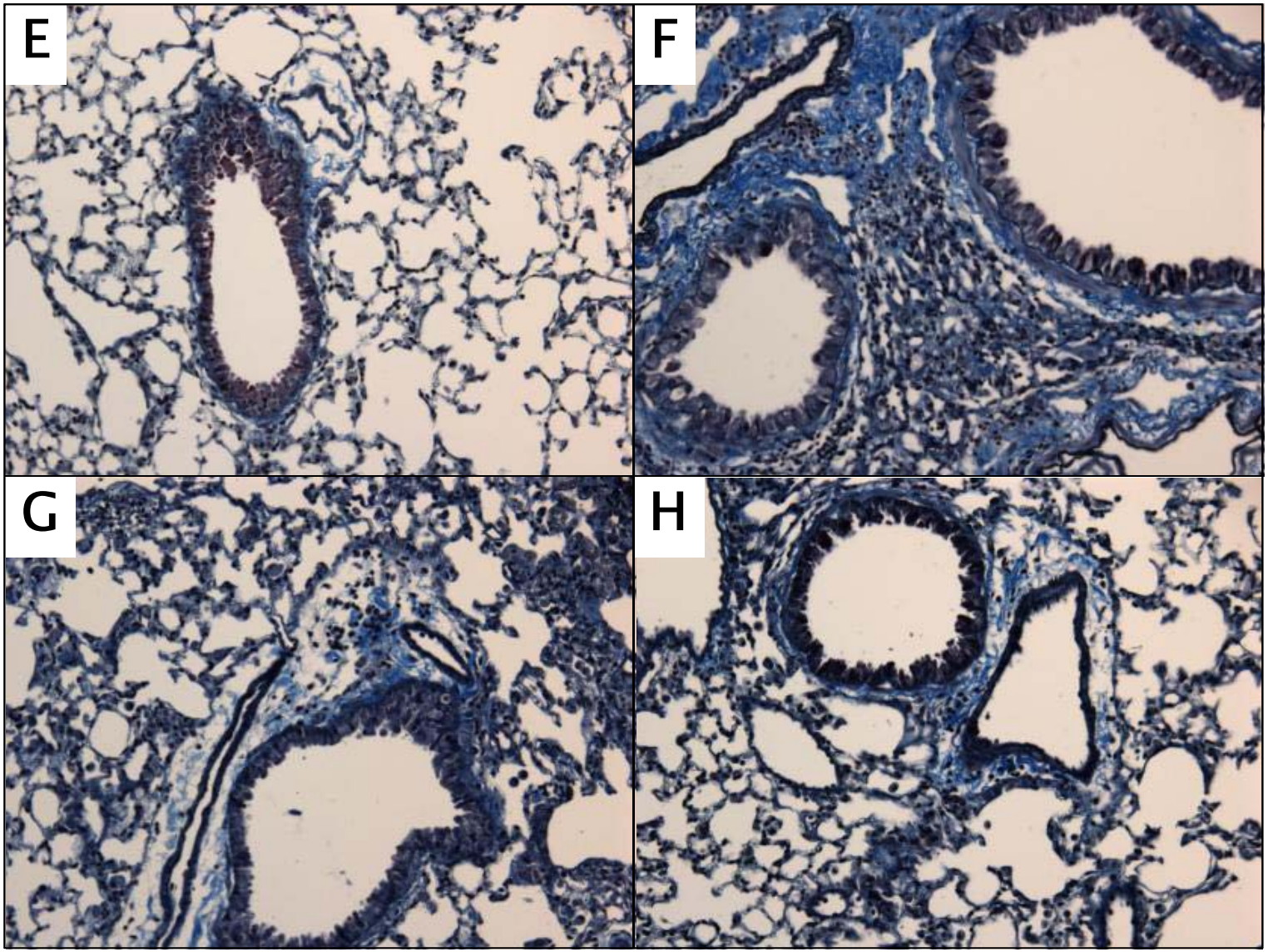

Figure 7

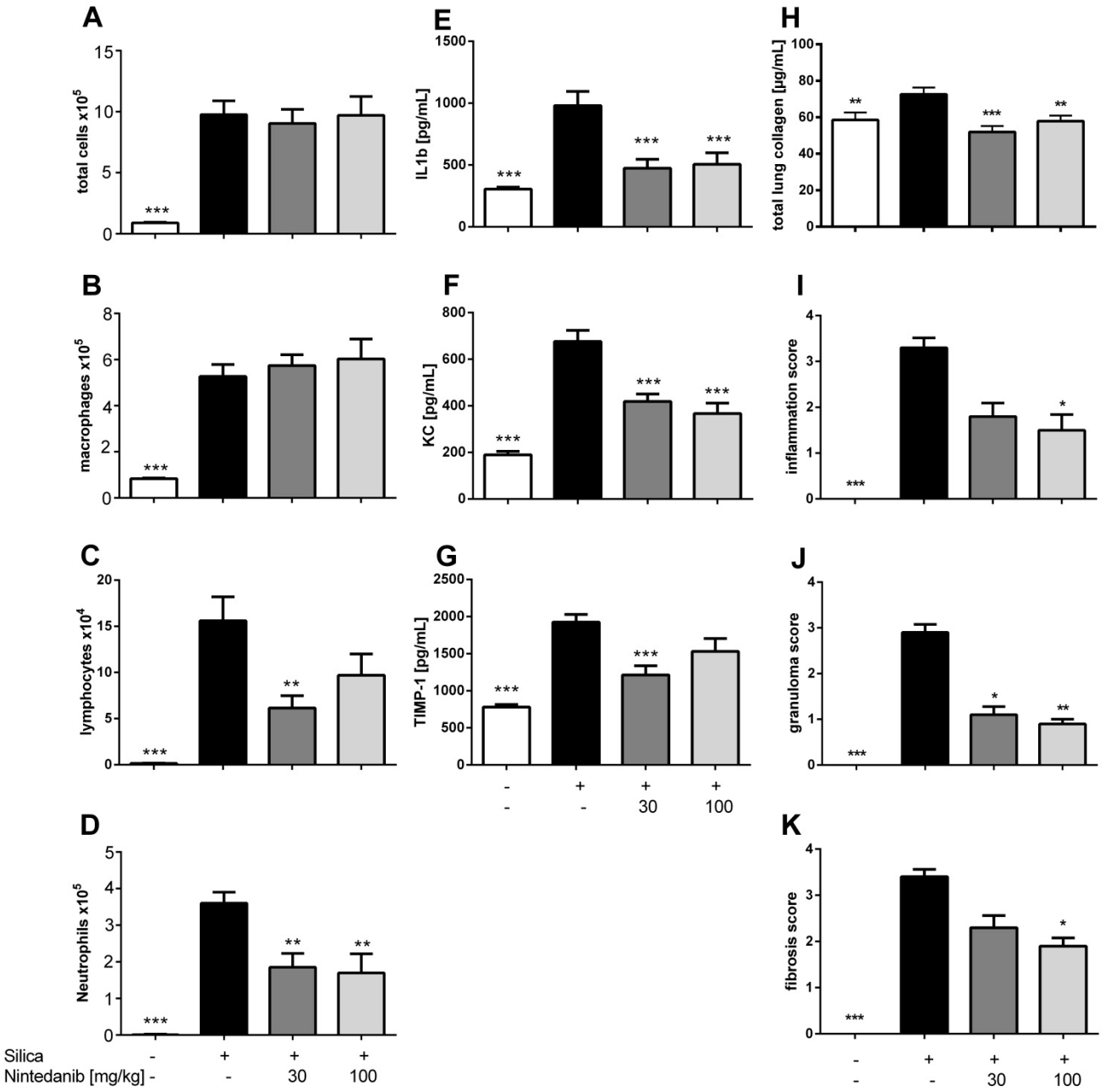
A
total cells x10^5
B
macrophages x10^5
C
lymphocytes x10^4
D
Neutrophils x10^5
E
IL1b [pg/mL]
F
KC [pg/mL]
G
TIMP-1 [pg/mL]
H
total lung collagen [µg/mL]
I
inflammation score
J
granuloma score
K
fibrosis score
Silica - + + +
Nintedanib [mg/kg] - - 30 100

Figure 8

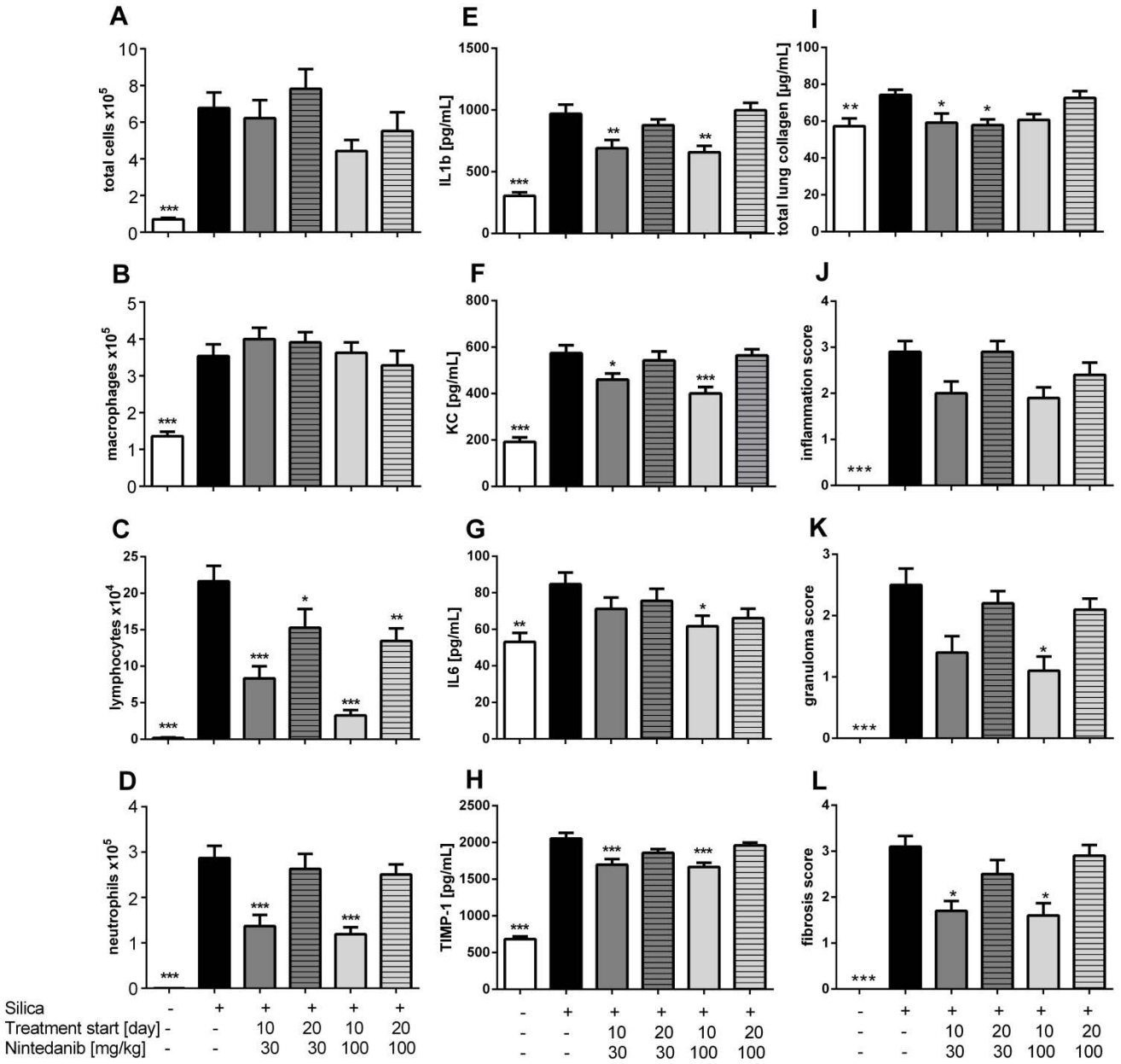
A
total cells x10^5
B
macrophages x10^5
C
lymphocytes x10^4
D
neutrophils x10^5
E
IL1b [pg/mL]
F
KC [pg/mL]
G
IL6 [pg/mL]
H
TIMP-1 [pg/mL]
I
total lung collagen [µg/mL]
J
inflammation score
K
granuloma score
L
fibrosis score
Silica - + + + + +
Treatment start [day] - - 10 20 10 20
Nintedanib [mg/kg] - - 30 30 100 100